CrossMark

SHORT COMMUNICATION

Electrocatalytic oxidation of urea on a sintered Ni–Pt electrode

Ewelina Urbańczyk[1] · Artur Jaroń[2] · Wojciech Simka[1]

Abstract Urea is present in the environment as a result of large amounts of wastewater from various origins. One of the most effective methods for disposing of urea involves electrochemical oxidation. This study investigated the use of sintered Ni–Pt electrodes as anodes in the electrocatalytic oxidation of urea. The activity of the Ni–Pt electrodes was compared with those of conventional Ti/Pt and Ni electrodes. Based on our results, the sintered Ni–Pt electrodes exhibited much higher activity in the oxidation of urea compared with the conventional anodes.

✉ Wojciech Simka
  wojciech.simka@polsl.pl

[1] Electrochemistry Group, Faculty of Chemistry, Silesian University of Technology, B. Krzywoustego Street 6, 44-100 Gliwice, Poland

[2] Faculty of Chemical Engineering and Technology, Cracow University of Technology, Warszawska Street 24, 31-155 Krakow, Poland

Springer

Graphical Abstract

A Ni–Pt electrode for electrocatalytic oxidation of urea
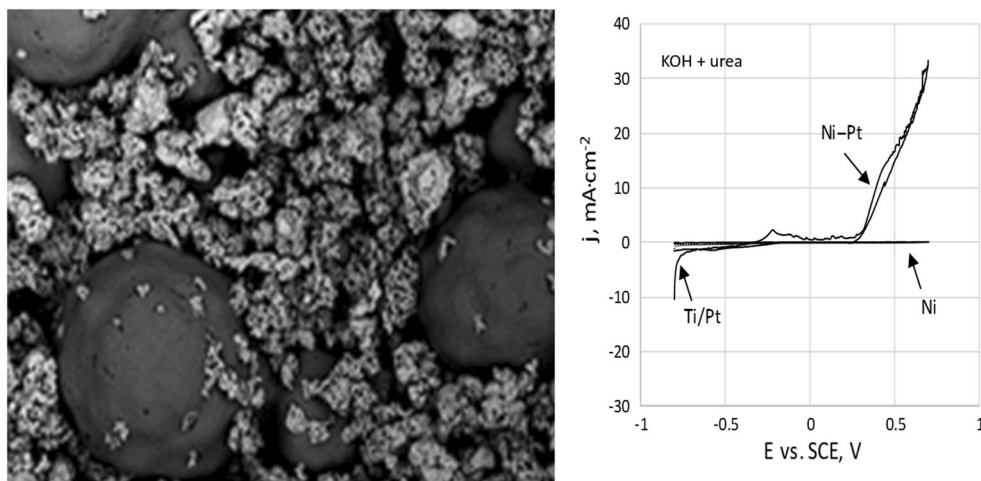
1 Introduction

Urea is an important chemical compound because of its
wide application in many industries. As one of the main
end products of metabolism in most animals, urea is pre-
sent in large quantities in the environment [1]. Another
source of urea is wastewater generated during the pro-
duction of urea [2, 3]. Wastewater containing urea can be
purified by various methods. Hydrolysis is employed most
often, but other methods, such as adsorption, chemical
oxidation, biological decomposition, and enzymatic
decomposition, have also been successfully applied. In
addition, electrochemical oxidation can be used to
decompose urea into non-toxic products, such as CO_2, N_2,
and H_2O [4]. The classical electrooxidation of urea can be
carried out using different anode materials (e.g., Ti/Pt and
Ti(RuO_2–TiO_2) electrodes) [4, 5]. In modern procedures
for urea electrooxidation, anodes with catalytic properties
are utilized. Electroactive anodes are primarily composed
of nickel-based materials [6].

The mechanism of the electrocatalytic oxidation of urea
was described in a previous study [7]. During the oxidation
of urea in alkaline media, nickel-based anodes exhibit
higher electrocatalytic activity than noble metals, such as
Pt, Ir, and Rh [7]. Different combinations of metals have
been investigated for use as nickel-based catalysts (e.g., Pt–
Ni, Rh–Ni, and Pt–Ir–Ni [8]; Ni–Co bimetallic hydroxide
[9]; and Ni–Zn and Ni–Zn–Co [10] graphene–nickel
nanocomposites) [11].

In this study, a sintered Ni–Pt electrode was employed
as the anode in the electrocatalytic oxidation of urea in an
alkaline solution. The effects of different scan rates during
cyclic voltammetry and various urea concentrations were
investigated. The activity of the new Ni–Pt electrode was
compared with that of Ni and Ti/Pt electrodes.

2 Experimental

A spherical nickel powder (Alfa Aesar) with 99.8% purity
and a grain-size distribution of 44–149 μm and a platinum
powder (Goodfellow) with 99.99% purity and irregular
grains that were 45 μm in size were used in the studies. A
porous nickel precursor was produced from the Ni powder
via oxidation (air) and reduction (mixture: H_2 at
333 mL h^{-1} + Ar at 83.5 mL h^{-1}) at 800 °C. Each of
these processes was carried out for 1.5 h [12–14]. Platinum
was deposited onto the surface of the prepared sinters,
where the pores were filled with nickel grains. In addition,
the excess Pt powder was removed (by sliding the edge of
the glass slide on the surface of the sinter) from the surface
of the electrode precursor. The nickel sinter with the
platinum deposit was subjected to oxidation in air and
reduction in an atmosphere consisting a H_2 + Ar mixture
(4:1$_{\text{vol}}$) for 1.5 h each at 800 °C [14] to produce Ni–Pt
sinters that were 8 mm in diameter and 2 ± 0.05 mm
thick. As earlier BET measurements indicated, the surface
area of such obtained metallic sinters may be approximated
by geometric surface [13, 21].

The electrochemical activity of the prepared electrode
was also compared with that of Ni (99, 99%) and Ti/Pt
electrodes. The Ti/Pt electrode was prepared by

electrodeposition of platinum on a titanium substrate. The electrodeposition process was conducted in an electrolyte based on *cis*-dinitrodiaminoplatinum (process time: 21 h; thickness of platinum layer: 3 µm).

The surface morphology and elemental composition of the Ni–Pt, Ni and Ti/Pt electrodes were examined using a scanning electron microscope (SEM, Phenom ProX) equipped with an energy dispersive X-ray (EDX) analysis system.

Electrochemical measurements of the Ni–Pt, Ni, and Ti/Pt electrodes were conducted in 1 M KOH (pH 14) (Chempur, Poland) in the presence of urea (Chempur, Poland) at different concentrations (0.00, 0.10, 0.33, and 0.50 M). The apparatus included a standard electrolysis cell with the following three electrodes: a working electrode, platinum auxiliary electrode, and Haber-Luggin capillary with a reference electrode (saturated calomel electrode, SCE). The electrolysis cell was powered by a potentiostat (PARSTAT 4000, Ametek) equipped with Versa Studio software. The investigations included the following measurements: (a) cyclic voltammetry from −0.8 to 0.7 V versus SCE at scan rates of 1, 10, 50, and 100 mV s^{-1} and (b) chronoamperometry at a constant potential of 0.5 V versus SCE for 1 h. The solution was not stirred during experiments.

3 Results and discussion

The SEM images of the Ni–Pt, Ni, and Ti/Pt electrodes are shown in Fig. 1. The structures of the electrode surfaces significantly differed from each other. On the surface of the Ni–Pt electrode, large spheres were composed of nickel, and smaller particles consisted of platinum (white areas). However, the morphologies of the Ti/Pt and Ni electrodes were much more homogeneous. Due to the extensive electrode surface, the Ni–Pt electrode was characterized by a much larger surface area compared to those of the conventional Ni and Ti/Pt electrodes.

The cyclic voltammograms of the Ni–Pt electrode in 1 M KOH in the absence of urea at different scan rates are shown in Fig. 2a. In the curves, two peaks are visible. The first peak was observed in the anodic region at 376 mV and corresponds to the oxidation of Ni^{2+} to Ni^{3+} ($Ni(OH)_2$ to $NiOOH$) [7]. The second peak was observed at 188 mV in the cathodic region and corresponds to the reduction of Ni^{3+} to Ni^{2+} ($NiOOH$ to $Ni(OH)_2$). During potential scanning in an alkaline solution, nickel can be oxidized to $Ni(OH)_2$, which can occur in two crystallographic phases (i.e., α-$Ni(OH)_2$ and β-$Ni(OH)_2$) [15, 16]. During scanning, α-$Ni(OH)_2$ forms first, and this phase is converted to the more stable β-$Ni(OH)_2$ with increasing time and potential. When the potential was further increased, β-$NiOOH$ formed. This form may be partially converted to γ-$NiOOH$, which collects on the surface of the electrode. The reduction peak may correspond to the transition of γ-$NiOOH$ to β-$Ni(OH)_2$ [17]. Analogical peaks to peaks recorded for the Ni–Pt electrode and corresponding to the oxidation/reduction reactions (Ni^{2+}/Ni^{3+}) were also present for the Ni electrode; however, their current density was much smaller. The Pt electrode in 1 M KOH exhibited neither oxidation nor reduction peaks in the studied potential range. The Ni–Pt electrode exhibited higher activity than the Ni and Ti/Pt electrodes (Fig. 2c). Except for the peaks corresponding to the oxidation and reduction of nickel compounds, a second peak corresponding to oxidation was observed at a potential of −199 mV. This peak may be due to the increased activity of the Ni–Pt electrode compared to the other monometallic electrodes and the adsorption of hydroxyl groups on the catalyst surface [18]. Higher activity of the Ni–Pt electrode can be related to a preparation process that includes a high-temperature oxidation and reduction.
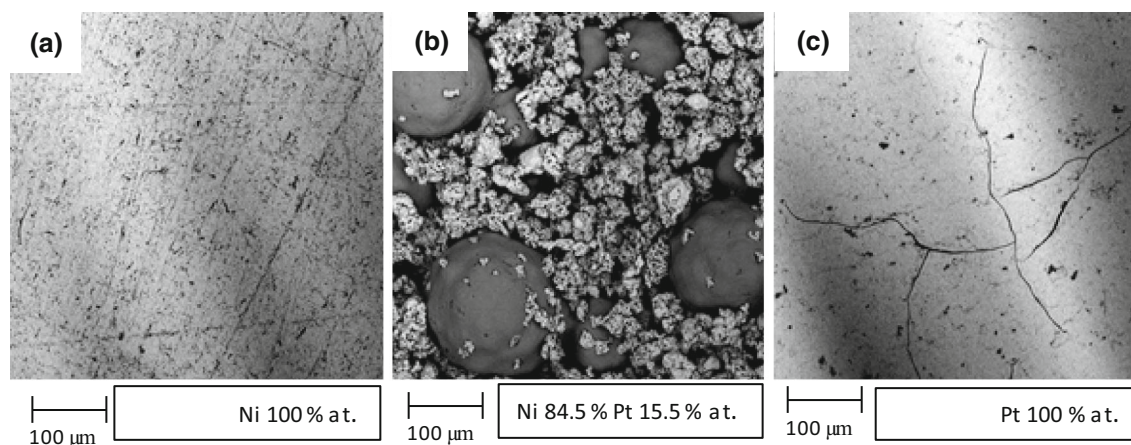

Fig. 1 SEM images of the electrodes and electrode characterization via EDX: **a** Ni, **b** Ni–Pt, and **c** Ti/Pt
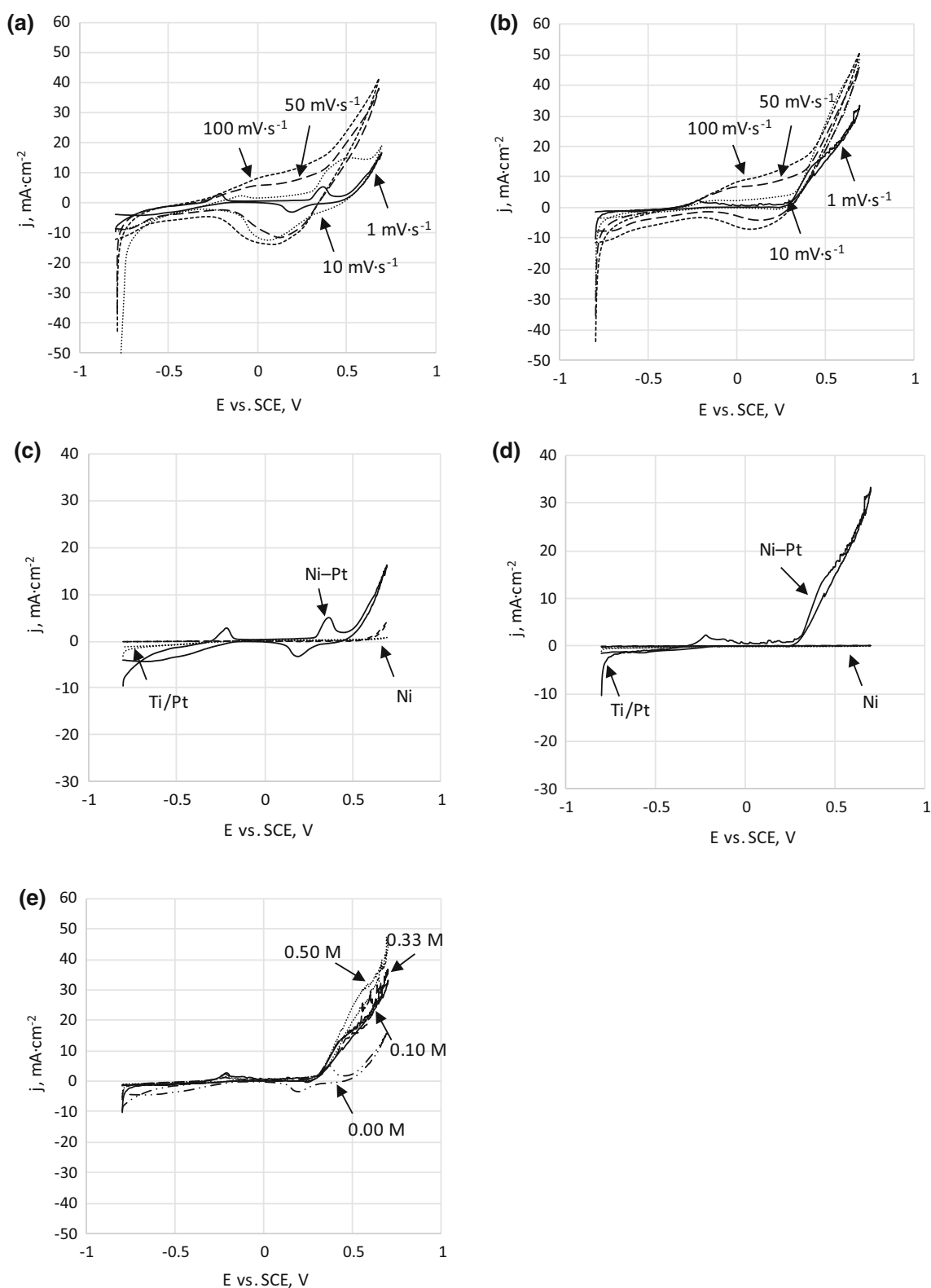
Fig. 2 Cyclic voltammograms of the **a** Ni–Pt electrode in 1 M KOH using different scan rates, **b** Ni–Pt electrode in 1 M KOH with the addition of 0.33 M urea using different scan rates, **c** Ni–Pt, Ni, and Ti/Pt electrodes in 1 M KOH at a scan rate of 1 mV s^{-1}, **d** Ni–Pt, Ni, and Ti/Pt electrodes in 1 M KOH with the addition of 0.33 M urea at a scan rate of 1 mV s^{-1}, and **e** Ni–Pt electrode in 1 M KOH with the addition of 0.00, 0.10, 0.33, and 0.50 M urea at a scan rate of 1 mV s^{-1}

The influence of the scan rate on the electrocatalytic oxidation of urea was also investigated. For the Ni–Pt electrode, an increase in the scan rate resulted in an increase in the anodic current density. Based on the curve shape, it was concluded that the urea oxidation reaction on the electrode surface is not reversible. The shift in the anodic peak potential to a positive value indicates a change in the reaction kinetics between urea and Ni^{3+}. This shift may have been caused by the adsorption of urea on the surface of the electrode where the Ni^{3+} reaction occurs [17, 19].

In the presence of urea (0.33 M), the curves obtained during cyclic voltammetry were similar to those obtained in KOH. However, the oxidation peak for the conversion of $Ni(OH)_2$ to NiOOH was less visible (Fig. 2b) due to the overlap of the anodic oxidation of $Ni(OH)_2$ to NiOOH and the oxidation of urea. At higher scan rates, the small reduction peak for the conversion of γ-NiOOH to β-$Ni(OH)_2$ was also visible. At a scan rate of 1 mV s^{-1}, an anodic peak at −199 mV was observed. In 1 M KOH with the addition of 0.33 M urea (Fig. 2d), the Ni–Pt electrode exhibited higher activity compared to the other electrodes. The presence of urea led to an increase in the anodic current density at potentials higher than 300 mV.

The urea concentration did not have a large impact on the activity of these electrodes (Fig. 2e). The higher current density indicates that the curve was obtained in the presence of a higher urea concentration. This effect may have been caused by the high surface area of the Ni–Pt electrode. The surface area and location of the Ni^{3+} species on the surface were sufficient to oxidize urea molecules, and these species were not blocked by the oxidation products.

Compared to the Ni and Ti/Pt electrodes, the Ni–Pt electrode was characterized by higher current during chronoamperometric measurements as well as higher activity in the urea oxidation process (Fig. 3). During chronoamperometry, the current decreased as a function of the measurement time, which is often caused by rapid wearing of the active electrode surface when the solution is not stirred [20]. In solution in the absence and presence of urea, the obtained curves for the Ni–Pt electrode were characterized by high stability during the measurement, which indicates the good electroactivity of this electrode in the electrocatalytic oxidation of urea.

4 Conclusions

A sintered Ni–Pt electrode was prepared and employed in electrochemical measurements to compare its activity in the electrocatalytic oxidation of urea with those of Ni and Ti/Pt electrodes. The Ni–Pt electrode was characterized by a high surface area. In 1 M KOH, the voltammograms of
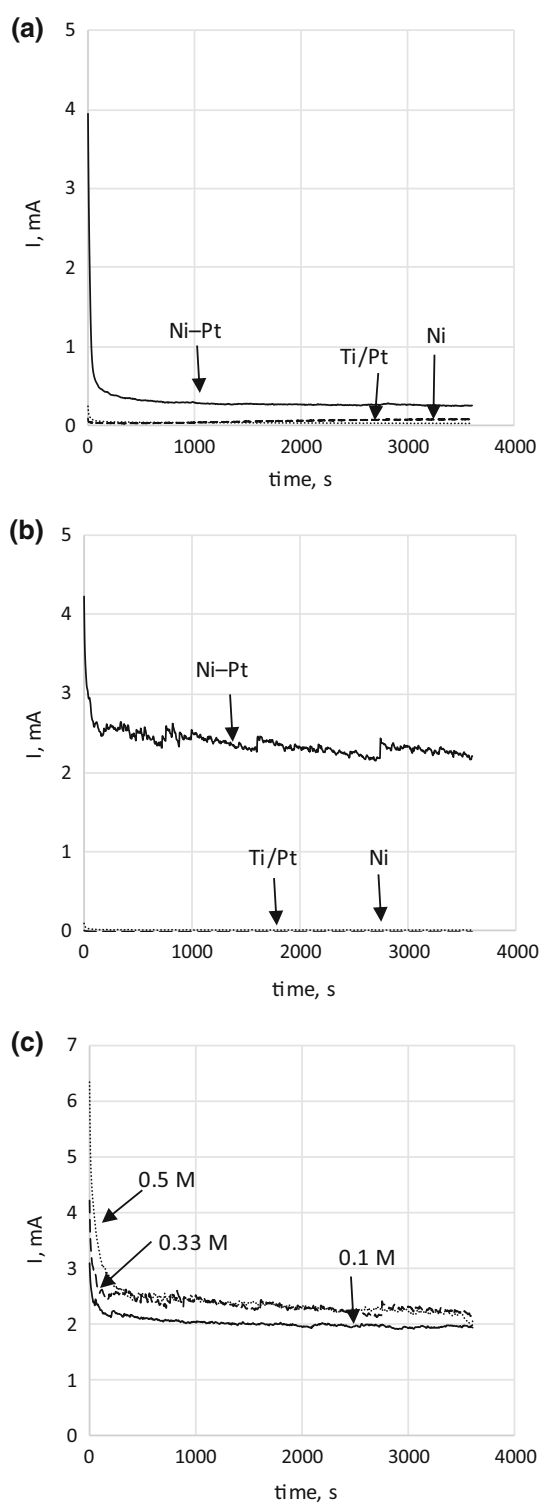

Fig. 3 Chronoamperograms of the **a** Ni–Pt, Ni, and Ti/Pt electrodes in 1 M KOH, **b** Ni–Pt, Ni, and Ti/Pt electrodes in 1 M KOH with the addition of 0.33 M urea, and **c** Ni–Pt electrode in 1 M KOH with the addition of 0.1, 0.33, and 0.5 M urea

the sintered Ni–Pt electrode were characterized by peaks corresponding to the oxidation of Ni^{2+} to Ni^{3+} as well as peaks in the cathodic region corresponding to the reduction

of Ni^{3+} to Ni^{2+}. In the voltammograms of the solution with added urea, the anodic oxidation of $Ni(OH)_2$ to NiOOH and the oxidation of urea overlapped. In the electrochemical measurements (i.e., cyclic voltammetry and chronoamperometry), the sintered Ni–Pt electrode exhibited higher activity than the Ni and Ti/Pt electrodes and was successfully employed for the electrocatalytic oxidation of urea.

References

1. Urbańczyk E, Sowa M, Simka W (2016) Urea removal from aqueous solutions—a review. J Appl Electrochem 46:1011–1029
2. Rollinson AN, Jones J, Dupont V, Twigg MV (2011) Urea as a hydrogen carrier: a perspective on its potential for safe, sustainable and long-term energy supply. Energy Environ Sci 4:1216–1224
3. Rollinson AN, Rickett GL, Lea-Langton A, Dupont V, Twigg MV (2011) Hydrogen from urea-water and ammonia-water solutions. Appl Catal B 106:304–315
4. Simka W, Piotrowski J, Robak A, Nawrat G (2009) Electrochemical treatment of aqueous solutions containing urea. J Appl Electrochem 39:1137–1143
5. Carlesi Jara C, Giulio S, Fino D, Spinelli P (2008) Combined direct and indirect electroxidation of urea containing water. J Appl Electrochem 38:915–922
6. Wang D, Yan W, Botte GG (2011) Exfoliated nickel hydroxide nanosheets for urea electrolysis. Electrochem Commun 13:1135–1138
7. Boggs BK, King RL, Botte GG (2009) Urea electrolysis: direct hydrogen production from urine. Chem Commun 32:4859–4861
8. King RL, Botte (2011) Hydrogen production via urea electrolysis using a gel electrolyte. J Power Sources 196:9579–9584
9. Yan W, Wang D, Botte GG (2012) Nickel and cobalt bimetallic hydroxide catalysts for urea electro-oxidation. Electrochim Acta 61:25–30
10. Yan W, Wang D, Botte GG (2012) Electrochemical decomposition of urea with Ni-based catalysts. Appl Catal B 127:221–226
11. Wang D, Yan W, Vijapur SH, Botte GG (2013) Electrochemically reduced graphene oxide–nickel nanocomposites for urea electrolysis. Electrochim Acta 89:732–736
12. Werber T, Żurek Z, Jaroń A (2008) The phenomena of adherence of a growing scale with inert materials under given reaction conditions. ECS Trans 16:109–121
13. Jaroń A, Żurek Z (2013) Electrochemical properties of electrode obtained by cyclic oxidation and reduction of Ni powder. ECS Trans 45:89–95
14. Jaroń A, Żurek Z, Stawiarski A (2015) Ni–Pt sintered electrode for hydrogen evolution from alkaline solutions. Ochr Przed Kor 58:381–383
15. Desilvestro J, Corrigan DA, Weaver MJ (1988) Characterization of redox states of nickel hydroxide film electrodes by in situ surface Raman spectroscopy. J Electrochem Soc 135:885–892
16. Van der Ven A, Morgan D, Meng YS, Cederc G (2006) Phase stability of nickel hydroxides and oxyhydroxides. J Electrochem Soc 153:A210–A215
17. Vedharathinam V, Botte GG (2012) Understanding the electrocatalytic oxidation mechanism of urea on nickel electrodes in alkaline medium. Electrochim Acta 81:292–300
18. Wanga J, Cheng N, Norouzi Banis M, Xiao B, Riese A, Sun X (2015) Comparative study to understand the intrinsic properties of Pt and Pd catalysts for methanol and ethanol oxidation in alkaline media. Electrochim Acta 185:267–275
19. Zhang J, Tse YH, Pietro WJ, Lever ABP (1996) Electrocatalytic activity of N,N',N'',N'''-tetramethyl-tetra-3,4-pyridoporphyrazinocobalt(II) adsorbed on a graphite electrode towards the oxidation of hydrazine and hydroxylamine. J Electroanal Chem 406:203–211
20. Yan W, Wang D, Diaz LA, Botte GG (2014) Nickel nanowires as effective catalysts for urea electro-oxidation. Electrochim Acta 134:266–271
21. Jaroń A, Żurek Z (2016) A porous nickel electrode designed for methanol oxidation. Ochr Przed Kor 59:98–101